

## Supporting Information

# Degradable Fluorescent Single-Chain Nanoparticles Based on Metathesis Polymers

Janin T. Offenloch,<sup>a,b</sup> Johannes Willenbacher,<sup>a,b</sup> Pavleta Tzvetkova,<sup>c</sup> Carolin Heiler,<sup>a,b</sup> Hatice Mutlu,<sup>\*a,b</sup> and Christopher Barner-Kowollik<sup>\*a,b,d</sup>

<sup>a</sup>Preparative Macromolecular Chemistry, Institut für Technische Chemie und Polymerchemie, Karlsruhe Institute of Technology (KIT), Engesserstr. 18, 76128 Karlsruhe, Germany,

<sup>b</sup>Soft Matter Synthesis Laboratory, Institut für Biologische Grenzflächen, Karlsruhe Institute of Technology (KIT), Hermann-von-Helmholtz-Platz 1, 76344 Karlsruhe, Germany.

<sup>c</sup>Institute of Organic Chemistry and Institute for Biological Interfaces 4 – Magnetic Resonance, Karlsruhe Institute of Technology (KIT), Fritz-Haber-Weg 6, 76131 Karlsruhe, Germany

<sup>d</sup>School of Chemistry, Physics and Mechanical Engineering, Queensland University of Technology (QUT), 2 George Street, QLD 4000, Brisbane, Australia

E-mail: hatice.mutlu@kit.edu, christopher.barner-kowollik@kit.edu, christopher-barnerkowollik@qut.edu.au

### **Content:**

A.	Experimental Procedures	S2
A.1.	Materials	S2
A.2.	Typical Procedure for the Synthesis of Acyclic Diene Metathesis Polymer	S2
A.3.	General Procedure for the Post-polymerization Modification of the ADMET Polymer	S3
A.4.	Typical Procedure for the Synthesis of Fluorescent Single-Chain Nanoparticles (SCNPs) via the Photoinduced Nitrile Imine Intramolecular Cross-Ligation	S4
A.5.	Degradation of the Single-Chain Nanoparticles	S5
B.	Measurements and Analysis	S7
B.1.	Nuclear Magnetic Resonance (NMR) Spectroscopy	S7
B.2.	Size Exclusion Chromatography (SEC)	S7
B.3.	Dynamic Light Scattering (DLS)	S8
B.4.	Ultraviolet-visible (UV-Vis) spectroscopy	S8
B.5.	Fluorescence spectroscopy	S8
B.6.	Diffusion-Ordered NMR Spectroscopy (DOSY)	S8
C.	Additional Data and Figures	S9
D.	References	S15

## A. Experimental Procedures

### A.1. Materials

Unless otherwise stated all chemicals were used as received. [1,3-bis-(2,4,6-trimethylphenyl)-2-imidazolidinylidene]dichloro(*o*-isopropoxy-phenylmethylene)ruthenium (97 %, second generation Hoveyda-Grubbs catalyst, HGII, Aldrich), *p*-Anisidine (Sigma Aldrich,  $\geq 99\%$ ), *o*-chlorobenzene (Acros, 99+ %), dichloromethane (DCM, Acros, 99.8 %, extra dry), 1,4-dioxane (Acros, 99+ %, extra pure), 4-dimethylaminopyridine (DMAP, Acros organics, 99 %), sodium dithionite (85 % technical grade,  $\text{Na}_2\text{S}_2\text{O}_4$ , Acros Organics), ethanol (VWR, normapur), ethanol amine (Acros, 99 %), 4-formylbenzoic acid (TCI, 98 %), furane (Acros, 99+ %, stabilized), hydrochloric acid (HCl, Roth, 37 %), magnesium sulfate ( $\text{MgSO}_4$ , Roth,  $\geq 99\%$ ), maleic anhydride (Acros, 99 %), pyridine (Sigma Aldrich, 99.8 % anhydrous), sodium nitrite ( $\text{NaNO}_2$ , Alfa Aesar, 98 %), succinic anhydride (Acros, 99 %), tetrahydrofuran (THF, VWR, 99.7 %, stabilized with BHT for SEC), tetrahydrofuran (THF, Acros, 99.5 %, extra dry, stabilized), toluene (VWR, normapur), *p*-toluenesulfonyl hydrazide (Alfa Aesar, 98 %), triethylamine (Fischer Scientific, 99 %), chloroform- $d_1$  ( $\text{CDCl}_3$ , Sigma Aldrich, 99.8 % D), dimethyl sulfoxide- $d_6$  ( $\text{DMSO}-d_6$ , eurisotop, 99.8 % D), tetrahydrofuran- $d_8$  ( $\text{THF}-d_8$ , Roth, 99.5 % D). Dichloromethane (DCM, VWR, normapur) was purified by rotary evaporation prior to photoinduced chain collapse. Synthesis of 4-(2-(1,3-dioxo-1,3,3a,4,7,7a-hexahydro-2H-4,7-epoxyisoindol-2-yl)ethoxy)-4-oxobutanoic acid (PG-Mal),<sup>1, 2</sup> 4-(2-(4-methoxyphenyl)-2H-tetrazol-5-yl)benzoic acid (Tet),<sup>3</sup> and (*E*)-(diazene-1,2-diylbis(4,1-phenylene))bis(methylene) di(undec-10-en-1-yl) bis(carbonate)<sup>4</sup> were synthesized according to literature procedures.

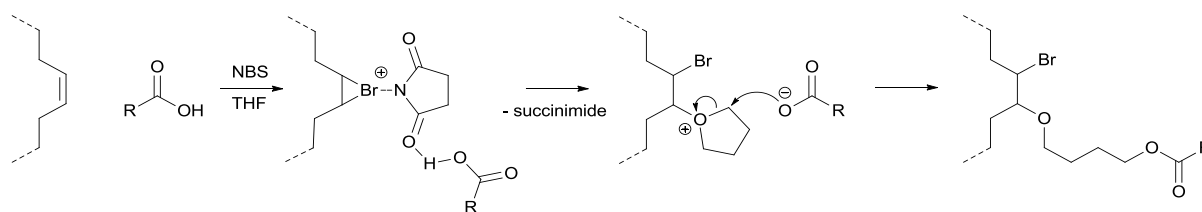
### A.2. Typical Procedure for the Synthesis of Acyclic Diene Metathesis Polymer.

The ADMET polymerization of the monomer was performed according to literature.<sup>4</sup> (*E*)-(diazene-1,2-diylbis(4,1-phenylene))bis(methylene) di(undec-10-en-1-yl) bis(carbonate) was polymerized in *o*-chlorobenzene as solvent. 261.5 mg (0.41 mmol) of monomer was dissolved in 686.5  $\mu\text{L}$  *o*-chlorobenzene (0.6 M) in a 10 mL flask which was evacuated (200 mbar vacuum and 65 °C). After 10 min, 5.2 mg HGII ( $\sim 8.30 \cdot 10^{-3}$  mmol, 2.0 mol% / molecule, *i.e.* 1.0 mol% / double bonds) were added, and the reaction was started at 65 °C under 200 mbar pressure with 500 rpm stirring. For the first 30 min, the pressure was kept at 200 mbar and the following 60 min at 100 mbar. The reaction was stopped after 90 min reaction time *via* dilution with 5 mL chloroform, and quenched *via* the addition of ethyl vinyl ether. Subsequently, the mixture was concentrated and precipitated in ice-cold methanol. The precipitate was collected by filtration, washed with ice-cold MeOH, and dried at ambient temperature.

**P1:**  $M_{n,\text{GPC}} = 12\,000\text{ g}\cdot\text{mol}^{-1}$ ,  $\bar{D} = 2.2$ .  $^1\text{H NMR}$  ( $\text{CDCl}_3$ , 500 MHz):  $\delta$  (ppm) = 7.91 (4 H, d,  $J = 8.3$  Hz,  $H_{\text{arom}}$  of the polymer backbone), 7.53 (4 H, d,  $J = 8.4$  Hz,  $H_{\text{arom}}$  of the polymer backbone), 5.42 – 5.31 (2 H, m,  $\text{CH}_2\text{CH}=\text{CHCH}_2$ ), 5.22 (4 H, s,  $\text{OCOCH}_2\text{Ph}$ ), 4.21 – 4.08 (4 H, m,  $\text{CH}_2\text{CH}_2\text{OCOO}$ ), 2.14 – 1.05 (32 H, m,  $\text{CHCH}_2\text{CH}_2\text{CH}_2\text{CH}_2\text{CH}_2\text{CH}_2\text{CH}_2\text{CH}_2\text{CH}_2\text{CH}_2\text{OCO}$ ).

### A.3. General Procedure for the Post-polymerization Modification of the ADMET Polymer.

The post-polymerization modification of ADMET with different loadings of the tetrazole and furane-protected maleimide acid derivatives (shown in Figure 1 in the Main Text) was performed in the following manner unless otherwise stated. Moreover, the mechanism of the post modification is depicted in Schemes S1. A typical procedure is illustrated here for the post-polymerization modification corresponding to **P1** in Scheme 1, adopting the conditions depicted in Table 1, Entry 3. Under anhydrous conditions, the ADMET polymer, tetrazole acid (Tet acid, 2.0 eq. with respect to the double bonds of the polymer backbone) and furane-protected maleimide acid (PG-Mal acid, 4.0 eq. with respect to the double bonds of the polymer backbone) were dissolved in dry THF and cooled to 0 °C. Subsequently, NBS (6.0 eq. with respect to the double bonds of the polymer backbone) was added, and the reaction mixture was stirred for 1 h at 0 °C. After 24 h at ambient temperature, the solvent was removed under reduced pressure. The residue was dissolved in THF, and the polymer was precipitated twice into cold MeOH, filtered off and dried under high vacuum to afford the polymer as a brown solid.

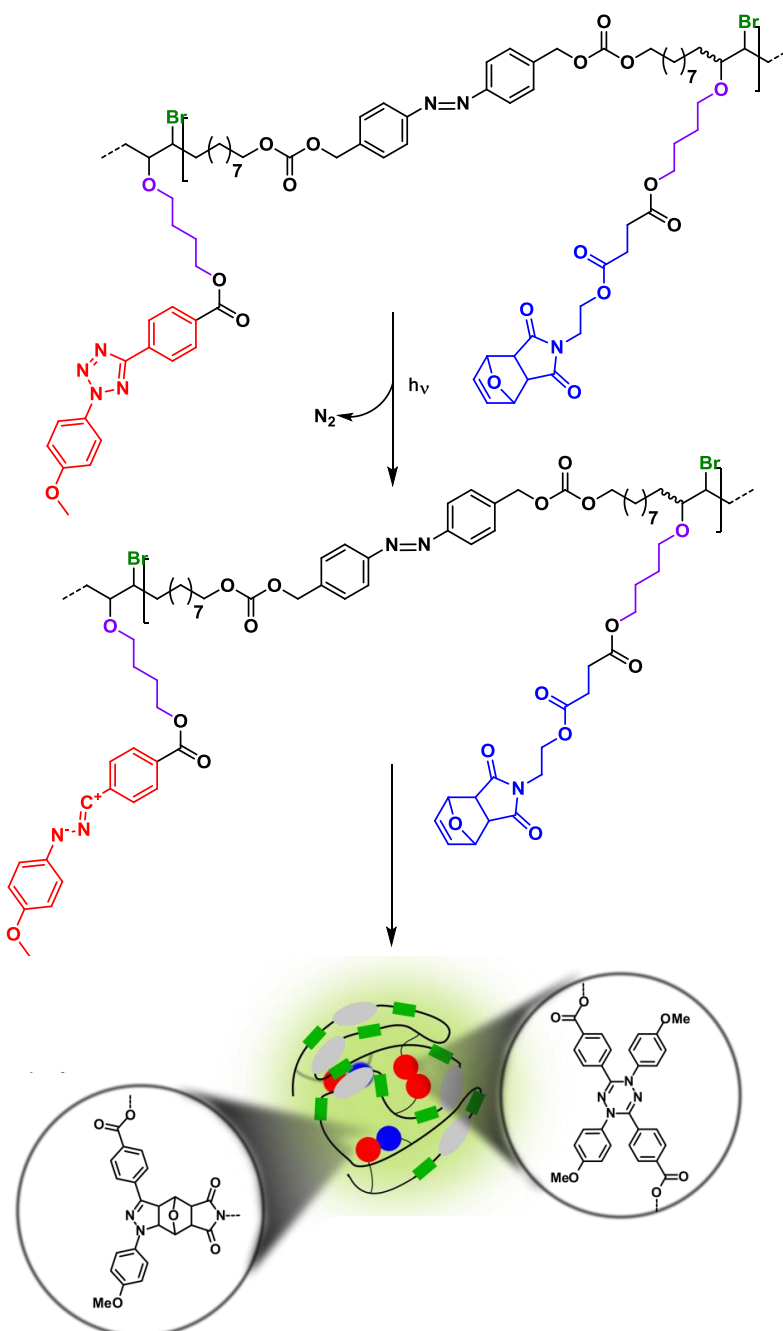


**Scheme S1** Proposed mechanism of the electrophilic alkoxyetherification reaction. The reaction pathway follows the formation of a cyclic bromonium ion starting from a carbon double bond and NBS. If a cyclic ether is employed as solvent, the ether opens the three-membered ring in a subsequent step. In the last step, the deprotonated carboxylic acid opens the cyclic ether. As a result, in the electrophilic alkoxyetherification the double bond is transformed into a carbon-bromine and an alkoxy bond, and the cyclic ether acts as a spacer between the former double bond and the acid, respectively. The yield of the presented multicomponent reaction strongly depends on the acidity of the carboxylic acid: The lower the  $pK_a$  value of the acid, the higher the yield. Furthermore, the reaction procedure tolerates radical scavenger and alcohols. Using the procedure, sulfonamides and amines can also be added to double bonds, and the formation of bromohydrines proceeds in analogous fashion.<sup>5,6,7,8</sup>

**P1.M:**  $M_{n,GPC} = 14\,900\text{ g}\cdot\text{mol}^{-1}$ ,  $\bar{D} = 2.0$ .  $^1\text{H NMR}$  ( $\text{CDCl}_3$ , 400 MHz):  $\delta$  (ppm) = 8.37 – 8.07 (6 H, m,  $H_{\text{arom}}$  of Tet), 7.91 (4 H, d,  $J = 8.0\text{ Hz}$ ,  $H_{\text{arom}}$  of the polymer backbone), 7.53 (4 H, d,  $J = 8.0\text{ Hz}$ ,  $H_{\text{arom}}$  of the polymer backbone), 7.09 – 7.05 (2 H, m,  $H_{\text{arom}}$  of Tet), 6.50 (2 H, s, unsaturated protons of PG-Mal), 5.25 (2 H, s,  $\text{CHO}$  of PG-Mal), 5.22 (4 H, s,  $\text{OCOCH}_2\text{Ph}$ ), 4.39 (1 H, m,  $\text{CHOCO}(\text{Tet/PG-Mal})$ ), 4.24 (2 H, t,  $J = 6.0\text{ Hz}$ ,  $\text{NCH}_2\text{CH}_2\text{OCO}$  of PG-Mal), 4.21 – 4.08 (4 H, m,  $\text{CH}_2\text{CH}_2\text{OCOO}$ ), 4.10 (1 H, m,  $\text{CHBr}$ ), 3.90 (3 H, s,  $\text{OCH}_3$  of Tet), 3.74 (2 H, t,  $J = 6.0\text{ Hz}$ ,  $\text{NCH}_2\text{CH}_2\text{OCO}$  of PG-Mal), 3.55 – 3.38 (2 H, m,  $\text{CHOCH}_2\text{CH}_2\text{CH}_2\text{CH}_2\text{OCO}$ ), 3.38 – 3.24 (1 H, m,  $\text{CH}_2\text{CHCHBr}$ ), 2.86 (2 H, s,  $\text{OCHCHCO}$  of PG-Mal), 2.70 – 2.52 (4 H, m,  $\text{OCOCH}_2\text{CH}_2\text{COO}$  of PG-Mal), 2.15 – 1.05 (32 H, m,  $\text{CHBrCH}_2\text{CH}_2\text{CH}_2\text{CH}_2\text{CH}_2\text{CH}_2\text{CH}_2\text{CH}_2\text{CH}_2\text{CH}_2\text{OCO}$ ).

#### A.4. Typical Procedure for the Synthesis of Fluorescent Single-Chain Nanoparticles (SCNPs) via the Photoinduced Nitrile Imine Intramolecular Cross-Ligation.

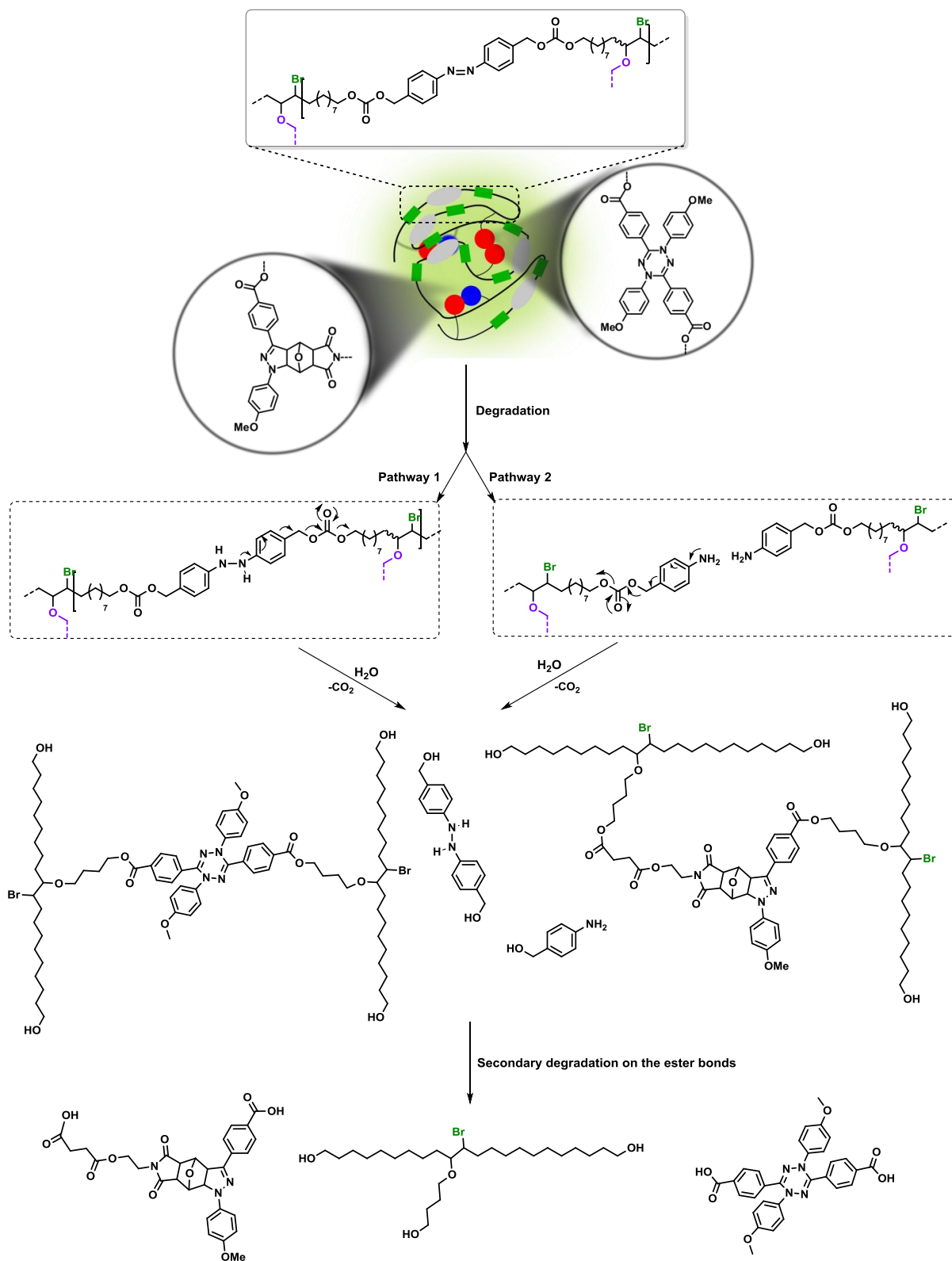
To fabricate SCNPs of **P1.M**, 36 mg of the functionalized ADMET polymer **P1.M** were dissolved in 1500 mL DCM and irradiated with UV light (Arimed B6 lamp, 36 W, see Figure S4) in a custom-built photoreactor (see Figure S5) for 30 min. Next, the reaction mixture was concentrated in vacuo and the formed **SCNPs** were precipitated in cold methanol. Filtration and drying under high vacuum afforded the product as a yellow solid. **SCNPs**:  $M_{n, GPC} = 8\ 900\ \text{g}\cdot\text{mol}^{-1}$ ,  $D = 2.2$ . Scheme S2 is showing the reaction pathway for the aforementioned synthesis of the SCNPs.



**Scheme S2** Reaction schemes for the NITEC ligation enabling the synthesis of the fluorescent SCNPs.

### A.5. Degradation of the Single-Chain Nanoparticles

Degradation reaction conditions were adopted from already reported procedures<sup>4,9,10</sup>. Thus, 20 mg of polymer SCNPs were dissolved in a mixture of 5 mL of THF<sub>tech. grade</sub> and 2 mL DCM<sub>tech. grade</sub>, and reacted with 500 mg (2.9 mmol) of sodium dithionite dissolved in 5 mL distilled water. The reaction mixture was stirred for 8 h at 37 °C under a continuous inert gas flow, while samples were periodically withdrawn to monitor the degradation. After 8 h, all solvents were removed and the residue dissolved in THF-d8. During the degradation reaction, the reaction mixture is heterogeneous due to the immiscibility of the employed solvents, thus the NMR spectra of the samples withdrawn at predetermined time intervals (refer to Figure S7, i.e. 1, 2, 3 and 4 h) are not quantitative. However, the last sample (at 8 h as shown in Figure S7, bottom spectrum) is representative of the entire reaction mixture. Thus, the <sup>1</sup>H NMR spectrum recorded after 8 h of degradation shows a slightly different spectrum in comparison to the earlier recorded spectra. The expected degradation pathway and the resulting products are depicted in Scheme S3. The degradation mechanism is assumed as follows: The treatment of the solution of SCNPs with an aqueous solution of sodium dithionite is expected to result in irreversible disruption of the SCNPs upon bond cleavage initiated by azobenzene reduction followed by self-immolative 1,6-elimination reactions. Indeed, with the addition of the reducing agent (i.e. sodium dithionite), the azobenzene functional group in each repeating unit of the SCNPs is first reduced either to the hydrazobenzene (**Pathway 1** in Scheme S3) or to the corresponding aniline derivative (**Pathway 2** in Scheme S3). It is well-known that the reduction of azobenzenes takes place in either a two-step fashion via the hydrazobenzene intermediate or both N-N bonds are severed simultaneously yielding aniline.<sup>11</sup> Thus, the generated hydrazobenzene and/or aniline derivatives are capable of a 1,6-elimination reaction due to the fact that both hydrazobenzene and aniline derivative contain an anilinic nitrogen, which can trigger the depolymerization of the SCNPs via the aforementioned 1,6-elimination-decarboxylation reaction. More specifically, the liberation of the aniline allows for elimination from the benzylic position to yield an azaquinone methide, which is subsequently trapped by water or another nucleophile to regenerate aniline. On the other hand, under the specified reaction conditions, it seems likely that non-specific hydrolytic cleavage occurred also on the ester bonds of the NITEC products, therefore affording the secondary degradation products presented in Scheme S3.



**Scheme S3** Reaction scheme depicting the pathway of degradation of the SCNPs in the presence of a reducing agent (i.e. sodium dithionite) and the resulting degradation products.

## B. Measurements and analysis:

**B.1. Nuclear Magnetic Resonance (NMR) spectroscopy.**  $^1\text{H}$  NMR spectra were recorded in  $\text{CDCl}_3$  on a Bruker Avance 500 MHz spectrometer equipped with Ultrashield magnets.  $^1\text{H}$  NMR chemical shifts are reported in ppm relative to the solvent's residual  $^1\text{H}$  signal. All NMR data were reported as follows: chemical shift, multiplicity (s = singlet, d = doublet, t = triplet, q = quartet), coupling constant(s) in Hertz (Hz) and integration. Multiplets (m) were reported over the range (ppm) where they appeared at the indicated field strength. In order to calculate the degree of polymerization ( $DP$ ) and the number average molecular weight ( $M_n$ ) of the ADMET polymers, we took advantage of the ratio of the proton resonances in the  $^1\text{H}$  NMR associated with the end groups ( $\text{E}_1$ - $\text{E}_3$ ) compared to the proton resonances of the methylene units  $-\text{OC}(\text{O})\text{O}-\text{CH}_2-(\text{CH}_2)_7-$  of the polymer chain in the  $^1\text{H}$  NMR spectra shown in Figure S1.<sup>4,12</sup> Three types of end groups can be detected in the final ADMET homopolymer polymer as a result of the olefin isomerization of the terminal double bonds:

$\text{E}_1$ :  $\text{CH}_3$ - end-group signals at 1.60 ppm ( $-\text{CH}_2=\text{CH}-\text{CH}_3$ ),

$\text{E}_2$ :  $\text{CH}_3$ - end-group at 0.88 ppm ( $-\text{CH}_2=\text{CH}-\text{CH}_2-\text{CH}_3$ ),

$\text{E}_3$ :  $\text{CH}_3$ - end-group at 0.96 ppm ( $-\text{CH}_2=\text{CH}-(\text{CH}_2)_n-\text{CH}_3$  with  $n \geq 2$ ).

Thus, the degree of polymerization ( $n$ ,  $DP$ ) was calculated using the integrals of the proton resonances of each end group: **A**, **B** and **C** are respectively the integral values of the resonances associated with end groups  $\text{E}_1$ ,  $\text{E}_2$  and  $\text{E}_3$ . In addition, **P** is the integral value associated with the proton resonances of the methylene units  $-\text{OC}(\text{O})\text{O}-\text{CH}_2-(\text{CH}_2)_7-$  of the polymer chain in the  $^1\text{H}$  NMR spectra:

$$n = DP = (3 \cdot P) / [(A + B + C) \cdot 2] \quad \text{Formula 1}$$

## B.2. Size Exclusion Chromatography (SEC)

The apparent number average molar mass ( $M_n$ ) and the molar mass distribution [ $D$  (polydispersity index) =  $M_w/M_n$ ] values of the polymers were determined using SEC measurements, which were performed on a TOSOH Eco-SEC HLC-8320 GPC System, comprising an autosampler, a SDV 5  $\mu\text{m}$  bead-size guard column (50  $\times$  8 mm, PSS) followed by three SDV 5  $\mu\text{m}$  columns (300  $\times$  7.5 mm, subsequently 100  $\text{\AA}$ , 1000  $\text{\AA}$  and  $10^5$   $\text{\AA}$  pore size, PSS), and Waters 2487 dual wavelength absorbance detector (analysis at 254 nm) in series with a refractive index detector using tetrahydrofuran (THF) as the eluent at 30  $^\circ\text{C}$  with a flow rate of 1  $\text{mL min}^{-1}$ . The SEC system was calibrated using linear polystyrene standards ranging from 266 to  $2.52 \cdot 10^6$   $\text{g mol}^{-1}$ . Calculation of the molecular weight proceeded via the Mark-Houwink-Sakurada (MHS) parameters for polystyrene (PS) in THF at 30  $^\circ\text{C}$ , i.e.,  $K = 13.63 \cdot 10^{-3} \text{ mL} \cdot \text{g}^{-1}$ ,  $\alpha = 0.714$ .

### B.3. Dynamic Light Scattering (DLS)

The apparent hydrodynamic diameters ( $D_{h,app}$ ) were determined at 25 °C by means of a dynamic light scattering (DLS) analysis using a Zetasizer Nano ZS light scattering apparatus (Malvern Instruments, UK) equipped with He-Ne laser (at a wavelength of 633 nm, 4 mW). The Nano ZS instrument incorporates a non-invasive backscattering (NIBS) optic with a detection angle of 173°. The polymer solutions were prepared in DCM, and were subsequently filtered into quartz cuvettes. The prepared samples were stabilized prior to DLS analysis at an ambient temperature. All values of the apparent hydrodynamic diameter for the polymer and the single-chain nanoparticles were averaged over triplicate measurements (11 runs/measurement), and were automatically provided by the instrument using a cumulative analysis.

### B.4. Ultraviolet-visible (UV-Vis) spectroscopy

UV-Vis spectra were recorded on a Biotek Epoch 2 spectrometer. Spectra were recorded in DCM at 20 °C with a concentration of 0.25 mg mL<sup>-1</sup>. Spectra were collected between 200 and 800 nm. Samples were baseline corrected with respect to the pure solvent.

### B.5. Fluorescence spectroscopy

Fluorescence spectra were measured on a Varian Cary Eclipse Fluorescence Spectrometer. All spectra were recorded in DCM ( $c = 40 \text{ mg L}^{-1}$ ) at 20 °C.

### B.6. Diffusion-Ordered NMR Spectroscopy (DOSY)

Diffusion-ordered spectroscopy experiments based on <sup>1</sup>H NMR were performed in THF-*d*<sub>8</sub> at 298 K on a Bruker 600 MHz Avance III spectrometer on a CPTCI inversely detected <sup>1</sup>H, <sup>13</sup>C, <sup>15</sup>N triple resonance cryogenically cooled probe head with actively shielded z-gradients, using a stimulated echo sequence incorporating bipolar gradient pulses and a longitudinal eddy current delay (BPP-LED)<sup>13</sup> with the standard Bruker pulse program, ledbpgp2s. The gradient strength was linearly incremented in 96 steps from 2 % up to 98 % of the maximum gradient strength. Diffusion times and gradient pulse durations were optimized for each experiment in order to achieve a 95% decrease in the signal intensities at the largest gradient amplitude. After Fourier transformation and phase correction, the diffusion dimension of the 2D DOSY spectra was processed by means of the Bruker Topspin software package (version 3.2) and analyzed with the Bruker Dynamic Center. Spectra for the single-chain nanoparticles were measured and mean values were taken from the found diffusion coefficients of characteristic NMR-peaks (see Figures S6a,b). For the single-chain nanoparticles, a mean value of  $2.77 \cdot 10^{-10} \text{ m}^2 \text{ s}^{-1}$  for the diffusion coefficient ( $D$ ) was determined. By the application of the Stokes-Einstein equation (eq.1), the hydrodynamic radius can be obtained:

$$r = \frac{k_B T}{6 \pi \eta D} \quad \text{Equation 1}$$

With  $\eta$  as viscosity of the applied solvent (THF:  $\eta = 0.4810 \text{ mPa s}^{-1}$ )<sup>13, 14</sup>



### C. Additional Data and Figures

**Table S1.** Results of the post-polymerization modification of the ADMET polymer. Conditions of the electrophilic alkoxyetherification of the ADMET-polymer **P1** in THF. The reactions were performed in a similar manner as described in section A.3. The degree of functionalization was determined by integration of the signals at 7.00 ppm for Tet and at 6.43 ppm for PG-Mal and compared with the signal of the aromatic protons in the polymer backbone at 7.53 ppm in the  $^1\text{H}$  NMR spectrum.

Entry	Tetrazole acid (eq.)	Furan-protected maleimide acid (eq.)	NBS (eq.)	Total functionalization of the double bond (%)	Ratio of Tet (%)	Ratio of PG-Mal (%)
1	2	2	2	60	70	20
2	2	2	4	75	75	25
3	2	4	6	75	60	40

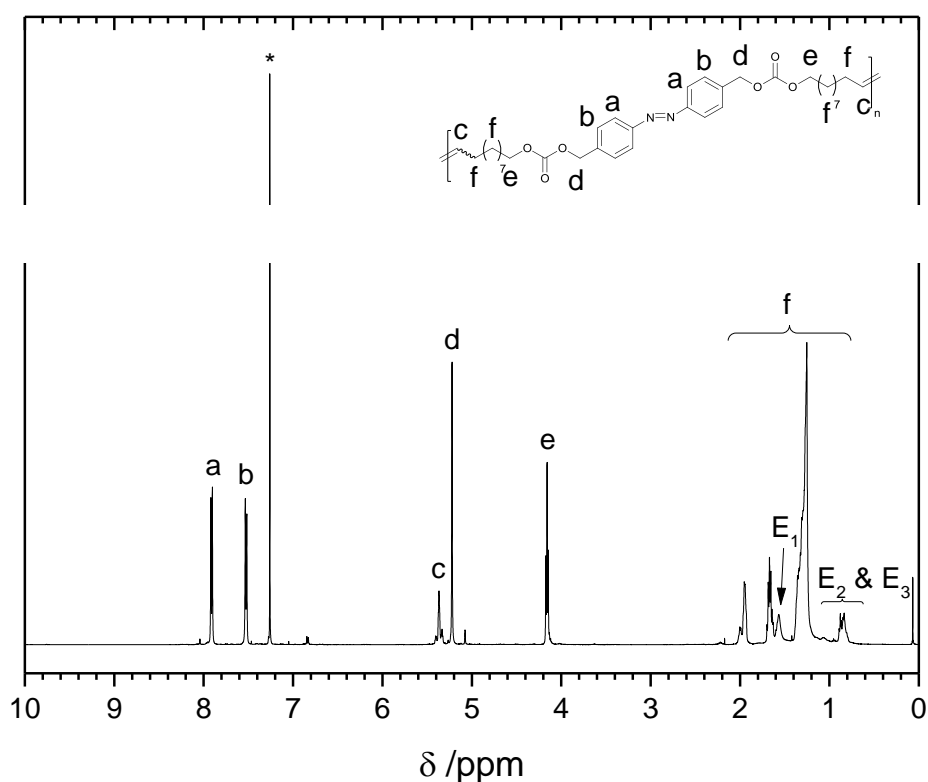


**Figure S1**  $^1\text{H}$  NMR (400 MHz) spectrum of the chain-shattering ADMET polymer **P1**. The peak marked with an asterisk can be assigned to  $\text{CDCl}_3$ .

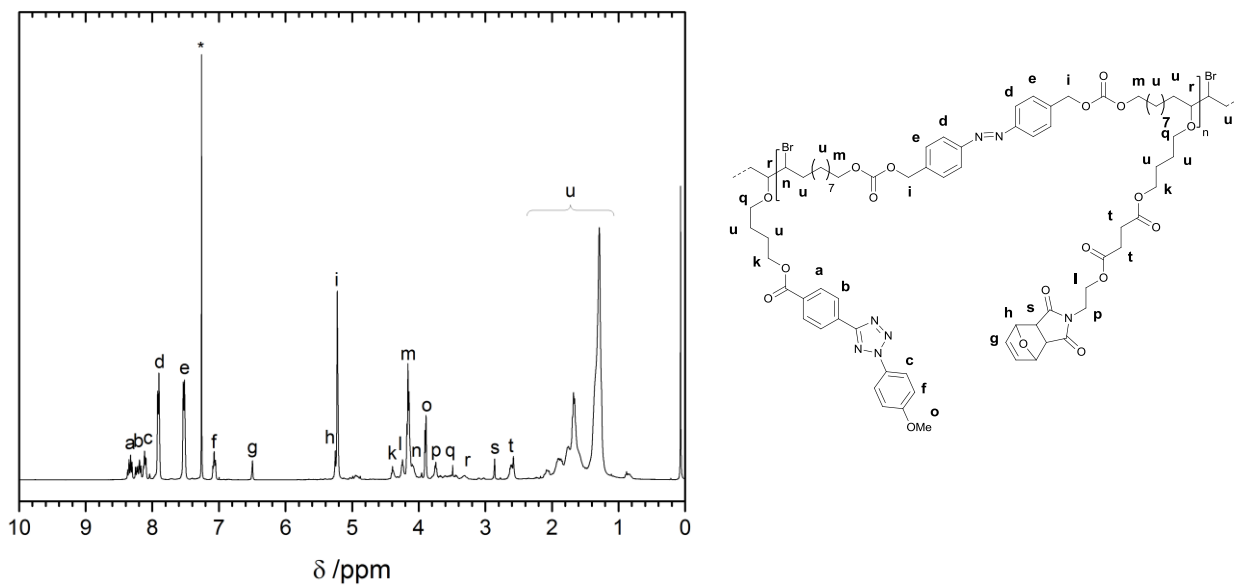


**Figure S2**  $^1\text{H}$  NMR spectrum (400 MHz,  $\text{CDCl}_3$ , at ambient temperature) and the representative structure of the modified ADMET polymer.

(a)

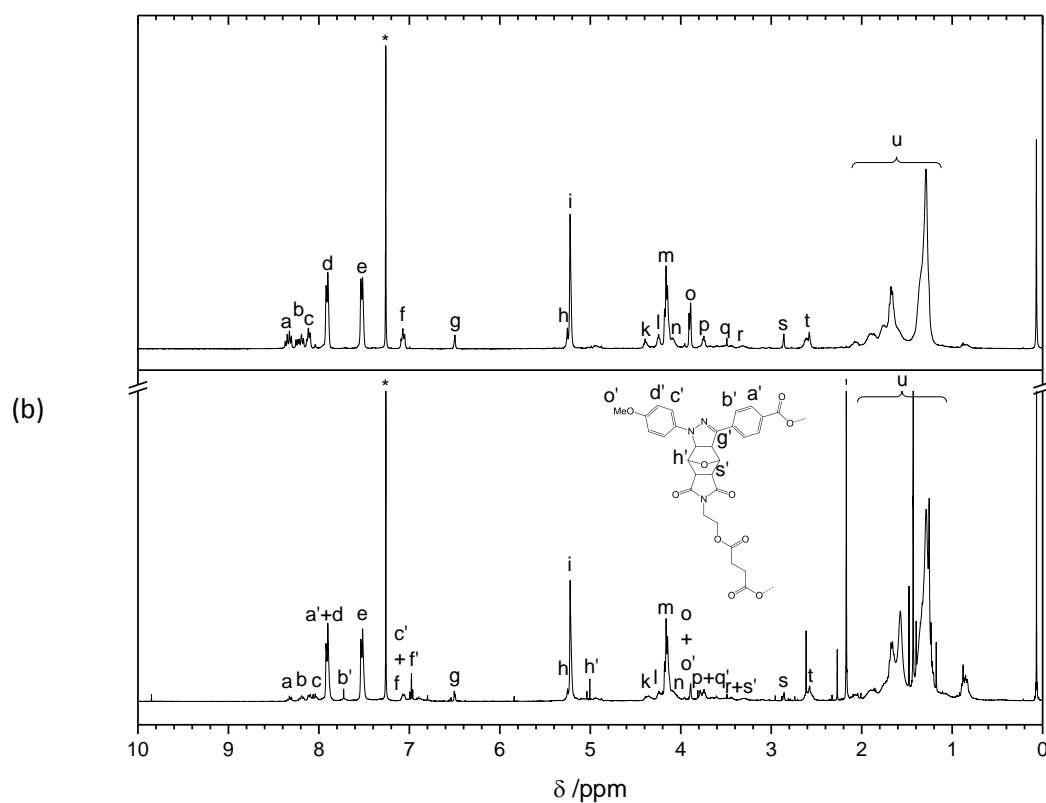


**Figure S3**  $^1\text{H}$  NMR spectrum (400 MHz) of the modified ADMET polymer (a) and the collapsed polymer chains (b) in  $\text{CDCl}_3$ .

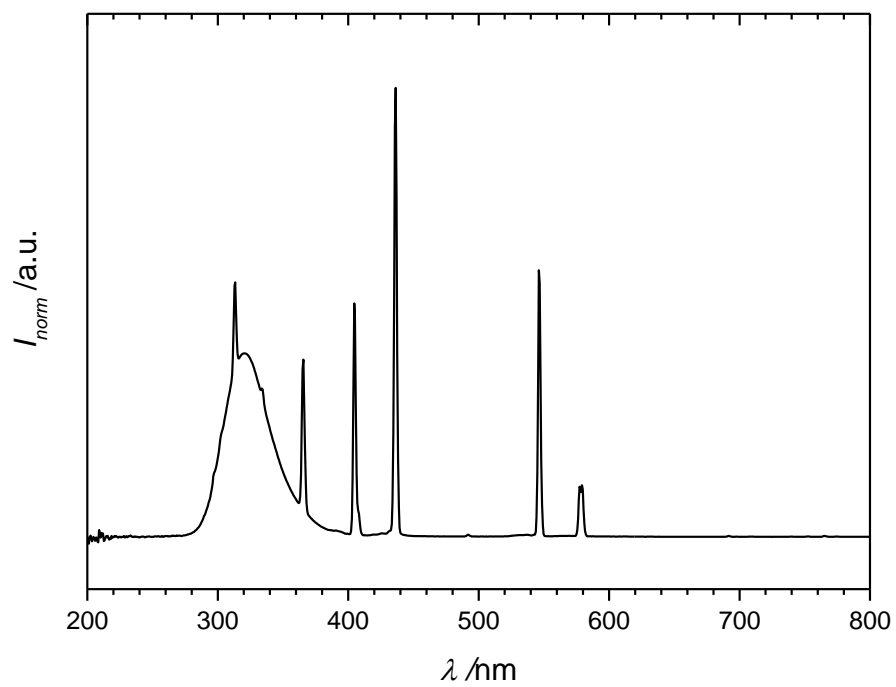


**Figure S4** Emission spectrum of the employed compact low pressure fluorescent lamp Arimed B6.

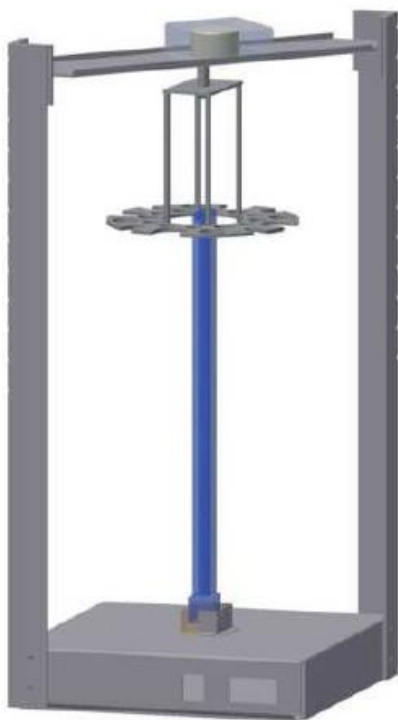


**Figure S5** Illustration of the custom-built photoreactor employed in the current study.

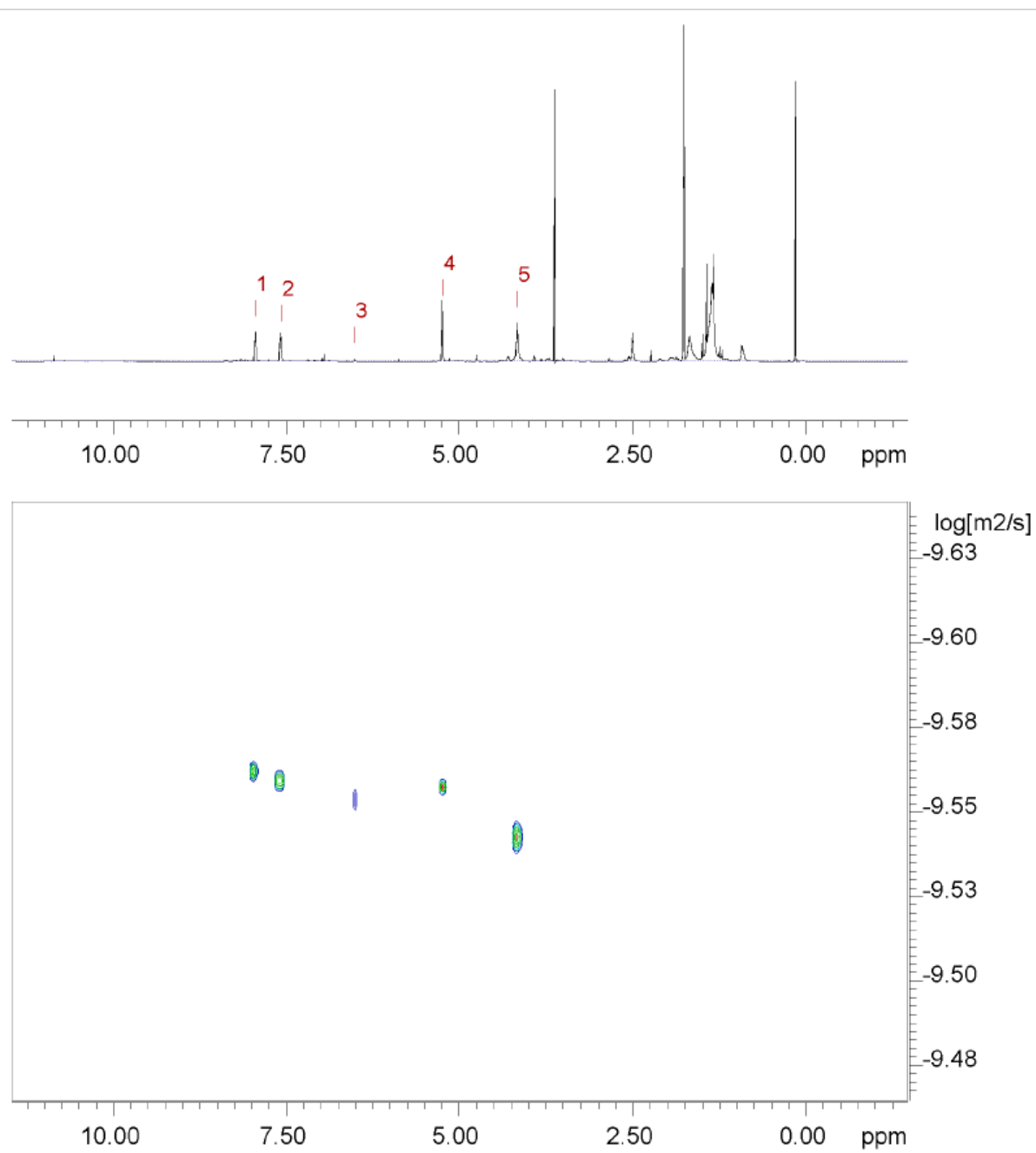


**Figure S6a** DOSY spectrum of the single-chain nanoparticles.

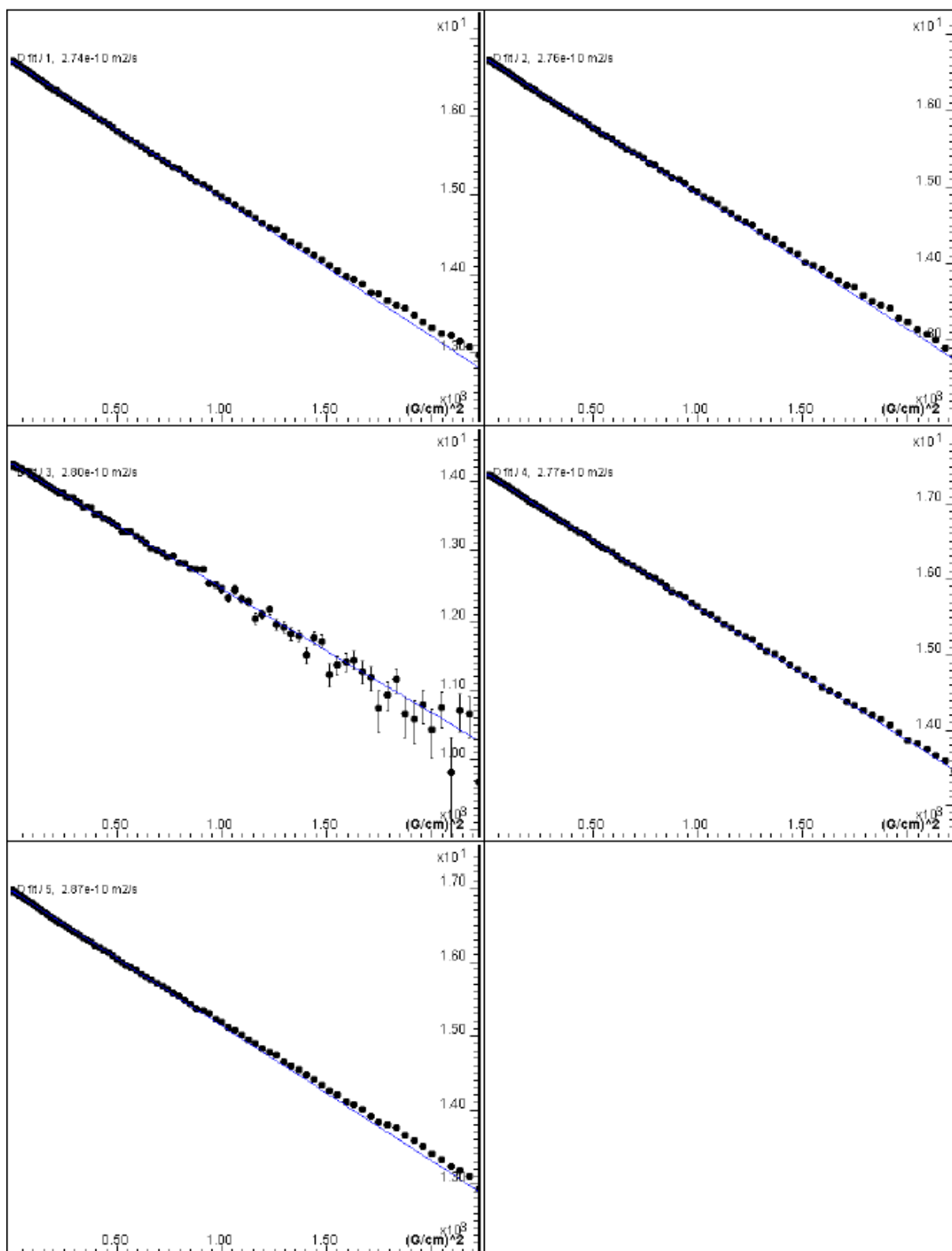


**Figure S6b** Fitting functions of the DOSY experiment of the single-chain nanoparticles.

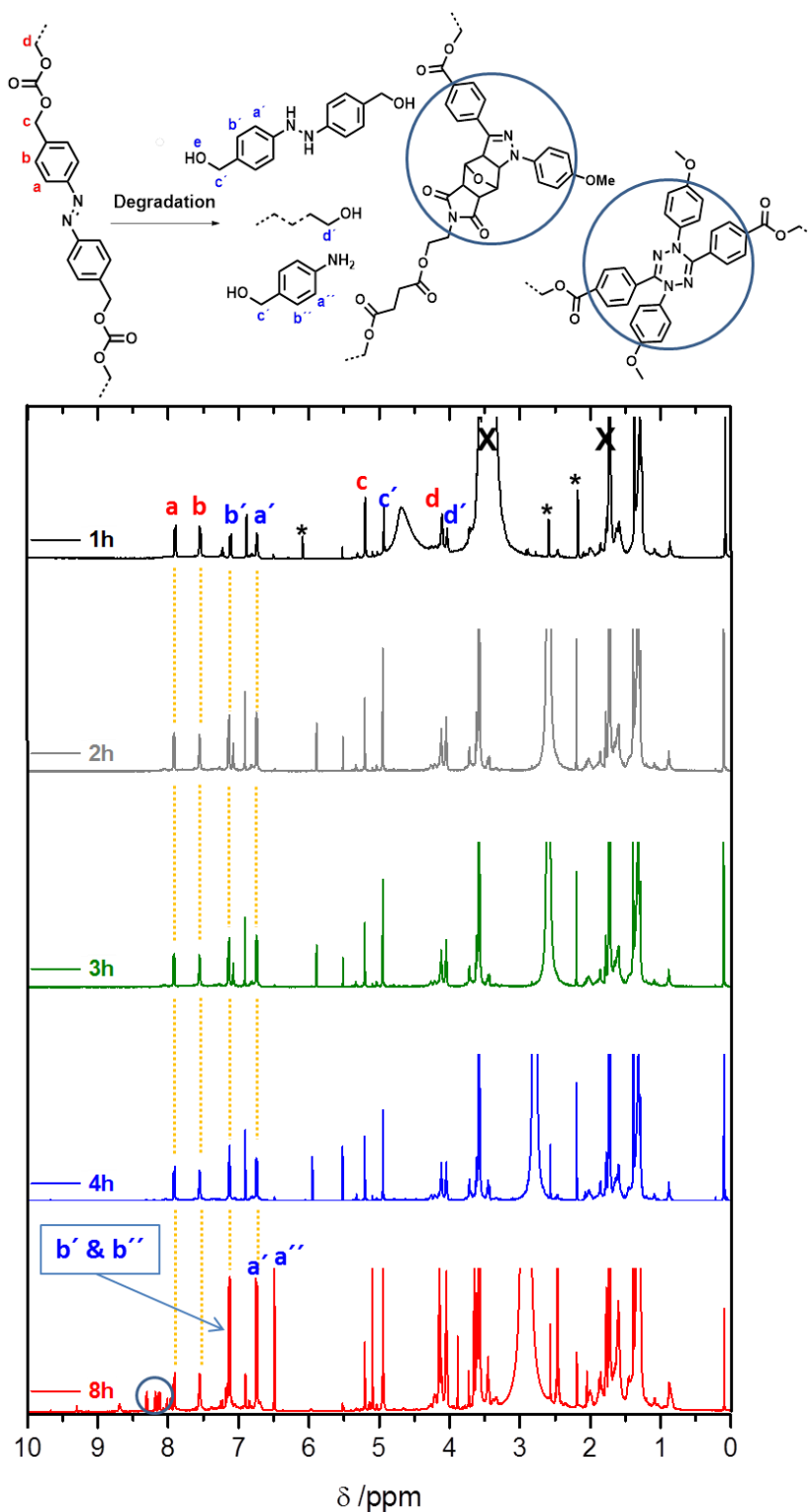


**Figure S7**  $^1\text{H-NMR}$  spectra (500 MHz,  $\text{THF-d}_8$ ) of the SCNPs degradation mixture withdrawn at the indicated predetermined time intervals. The spectral changes upon the reaction with a mild chemical trigger (i.e. sodium dithionite) provide evidence for the scission of the chain backbone of the SCNPs (magnetic resonances **a**, **b**, **c** and **d**) via the self-immolative degradation into small fragments (magnetic resonances **a'**, **b'**, **c'** and **d'**). The resonances of the NMR solvent residual ( $\text{THF-d}_8$ ) are indicated with "X", and "\*" are showing a contamination arising from the reaction mixture. The circle in the bottom 8h spectrum displays the resonances corresponding to the aromatic region of the NITEC linkage and the residual unreacted tetrazole units in the SCNPs system. The resonances corresponding to the aromatic region of 4-aminobenzyl alcohol are shown as **a''** and **b''**.

## D. References

- [1] G. Mantovani, F. Lecolley, L. Tao, D. M. Haddleton, J. Clerx, J. J. L. M. Cornelissen and K. Velonia, *J. Am. Chem. Soc.*, 2005, **127**, 2966-2973.
- [2] H. Durmaz, F. Karatas, U. Tunca and G. Hizal, *J. Polym. Sci., Part A: Polym. Chem.*, 2006, **44**, 3947-3957.
- [3] C. Rodriguez-Emmenegger, C. M. Preuss, B. Yameen, O. Pop-Georgievski, M. Bachmann, J. O. Mueller, M. Bruns, A. S. Goldmann, M. Bastmeyer and C. Barner-Kowollik, *Adv. Mater.*, 2013, **25**, 6123-6127.
- [4] H. Mutlu and C. Barner-Kowollik, *Polym. Chem.*, 2016, **7**, 2272-2279.
- [5] J. Chen, S. Chng, L. Zhou and Y.-Y. Yeung, *Org. Lett.*, 2011, **13**, 6456-6459.
- [6] C. K. Tan, W. Z. Yu and Y.-Y. Yeung, *Chirality*, 2014, **26**, 328-343.
- [7] P. Phukan, P. Chakraborty and D. Kataki, *J. Org. Chem.*, 2006, **71**, 7533-7537.
- [8] L. Zhou, C. K. Tan, J. Zhou and Y.-Y. Yeung, *J. Am. Chem. Soc.*, 2010, **132**, 10245-10247.
- [9] L. K. Sydnes, S. Elmi, P. Heggen, B. Holmelid and D. Malthe-Sørensen, *Synlett*, 2007, 1695-1698.
- [10] A. D. Wong, A. L. Prinzenb and E. R. Gillies, *Polym. Chem.*, 2016, **7**, 1871-1881.
- [11] R. Wiwattanapatapee, L. Lomlim, K. Saramunee, *J. Controlled Release*, 2003, **88**, 1-9.
- [12] A. Tüzün, G. Lligadas, J. C. Ronda, M. Galia and V. Cadiz, *Eur. Polym. J.*, 2015, **67**, 503-512.
- [13] D. Wu, A. Chen, and C. S. Johnson, *J. Magn. Reson. A*, 1995, **115**, 260-264.
- [14] T. M. Aminabhavi and B. Gopalakrishna, *J. Chem. Eng. Data*, 1995, **40**, 856-861.